esa ECOSPHERE

Quantifying spatially and temporally explicit CO_2 fertilization effects on global terrestrial ecosystem carbon dynamics

Shaoqing Liu,[1] Qianlai Zhuang,[1,2,†] Min Chen,[3] and Lianhong Gu[4]

[1]Department of Earth, Atmospheric, and Planetary Sciences, Purdue University, West Lafayette, Indiana 47907 USA
[2]Department of Agronomy, Purdue University, West Lafayette, Indiana 47907 USA
[3]Department of Global Ecology, Carnegie Institution for Science, Stanford, California 94305 USA
[4]Environmental Sciences Division, Oak Ridge National Laboratory, Oak Ridge, Tennessee 37831 USA

Citation: Liu, S., Q. Zhuang, M. Chen, and L. Gu. 2016. Quantifying spatially and temporally explicit CO_2 fertilization effects on global terrestrial ecosystem carbon dynamics. Ecosphere 7(7):e01391. 10.1002/ecs2.1391

Abstract. Current terrestrial ecosystem models are usually driven with global average annual atmospheric carbon dioxide (CO_2) concentration data at the global scale. However, high-precision CO_2 measurement from eddy flux towers showed that seasonal, spatial surface atmospheric CO_2 concentration differences were as large as 35 ppmv and the site-level tests indicated that the CO_2 variation exhibited different effects on plant photosynthesis. Here we used a process-based ecosystem model driven with two spatially and temporally explicit CO_2 data sets to analyze the atmospheric CO_2 fertilization effects on the global carbon dynamics of terrestrial ecosystems from 2003 to 2010. Our results demonstrated that CO_2 seasonal variation had a negative effect on plant carbon assimilation, while CO_2 spatial variation exhibited a positive impact. When both CO_2 seasonal and spatial effects were considered, global gross primary production and net ecosystem production were 1.7 Pg C·yr^{-1} and 0.08 Pg C·yr^{-1} higher than the simulation using uniformly distributed CO_2 data set and the difference was significant in tropical and temperate evergreen broadleaf forest regions. This study suggests that the CO_2 observation network should be expanded so that the realistic CO_2 variation can be incorporated into the land surface models to adequately account for CO_2 fertilization effects on global terrestrial ecosystem carbon dynamics.

Key words: atmospheric CO_2; carbon dynamics; gross primary production; net ecosystem production; process-based ecosystem model.

Received 4 November 2015; revised 17 March 2016; accepted 23 March 2016. Corresponding Editor: K. Johnson.

† **E-mail:** qzhuang@purdue.edu

Introduction

Increasing atmospheric carbon dioxide (CO_2) mainly due to the global consumption of fossil fuels has direct and indirect effects on the global terrestrial ecosystem carbon budget (Canadell et al. 2007). Numerous ecosystem-level experiments were conducted to understand how the terrestrial ecosystem carbon cycle responds to rising atmospheric CO_2 (e.g., Norby et al. 2002, Long et al. 2004, Ainsworth and Long 2005, Norby and Zak 2011). Land surface models have also been used to investigate the CO_2 fertilization effects on carbon dynamics (McGuire et al. 1993, Esser and Lautenschlager 1994, Pan et al. 1998, Gerber et al. 2004). However, these models were often driven with annual and uniformly distributed atmospheric CO_2 data (ESRL data set, http://www.esrl.noaa.gov/gmd/ccgg/trends/) at the global scale (Raich et al. 1991, White et al. 2000, Sitch et al. 2003, Krinner et al. 2005, Oleson et al. 2010, Lawrence et al. 2011).

Although atmospheric CO_2 is generally well mixed globally as it is chemically inert (Eby et al. 2009), it actually exhibits a large seasonal and spatial variability at the global scale (Miles et al. 2012, Zeng et al. 2014). The seasonal and spatial characteristics have previously been reported at site levels (Yi et al. 2000, 2004, Davis et al. 2003, Bakwin et al. 2004, Haszpra et al. 2008, Miles et al. 2012). For example, Yi et al. (2000) reported that the monthly averaged diurnal pattern of CO_2 mixing ratio at a forest site in northern Wisconsin could be as large as 70 ppmv in summer season (Yi et al. 2000). The summer measurement of atmospheric boundary layer CO_2 mole fraction from a nine-tower regional network conducted during the North American Carbon Program's Mid-Continent Intensive (MCI) during 2007–2009 showed that the seasonal CO_2 drawdown (25–38 ppm) was five times larger than the tropospheric background as represented by Mauna Loa observations. The spatial gradient (1.5 ppmv/100 km) across the MCI region was four times as large as the interhemispheric gradient (Miles et al. 2012). Similarly, the remote sensing data agree with data obtained from ground-based observations (Yang et al. 2002, Yokota et al. 2009). For example, Atmospheric Infrared Sounder (AIRS) and Greenhouse Gases Observing (GOSAT) satellite retrievals showed that the distribution of carbon dioxide differed significantly between the Northern Hemisphere (NH) and the Southern Hemisphere (SH) (Chahine et al. 2008, Yokota et al. 2009) and the column-averaged dry air mole fractions of CO_2 in NH were generally higher. The spatially varied atmospheric CO_2 exhibited the semiannual oscillation (Ruzmaikin et al. 2012) with the stronger seasonal variation in northern high latitudes as indicated by the GLOBALVIEW CO_2 and GEOS-Chem model simulations (Feng et al. 2011).

As CO_2 transformed into plant carbohydrates through leaf stomata is the initial step in carbon cycling, the accurate representation of CO_2 spatiotemporal variation is crucial for ecosystem modeling. Here we first derived the surface daily CO_2 measurement at four sites from Fluxnet to show the spatial and temporal variations in surface CO_2. Then the integrated Terrestrial Ecosystem Model (iTEM; Chen 2013, Liu et al. 2014) driven with two spatially and temporally explicit CO_2 data sets was used to analyze the atmospheric CO_2 fertilization effects on the global carbon dynamics of terrestrial ecosystems from 2003 to 2010.

Method

Overview

To reveal the spatial and temporal variations in atmospheric surface CO_2 concentrations, we first extracted the high-precision CO_2 measurement at four eddy flux tower sites from Fluxnet (http://fluxnet.ornl.gov/). Second, we carried out a simple test on the sensitivity of photosynthesis to the atmospheric CO_2 variation, using the coupled photosynthesis model with a stomatal function. Third, we conducted site-level tests to compare the simulated daily gross primary production (GPP) using the in situ CO_2 measurement with that using the uniformly distributed atmospheric CO_2 data. Finally, two spatially and temporally explicit CO_2 data sets were used to drive iTEM from 2003 to 2010 at the global scale. The two spatially and temporally explicit CO_2 data sets were obtained from the National Oceanic & Atmospheric Administration (NOAA) Carbon Tracker and Monitoring of Atmospheric Composition and Climate (MACC) project, respectively. In addition, we used mean annual CO_2 value computed from NOAA CO_2 and MACC CO_2 to quantify the effect of seasonal CO_2 variation on carbon dynamics. Totally, we had four simulations: (1) iTEM + NOAACO_2 (S1-NOAA), (2) iTEM + mean annual NOAACO_2 (S1-mNOAA), (3) iTEM + MACCCO_2 (S1-MACC), and (4) iTEM + mean annual MACCCO_2 (S1-mMACC). Therefore, the spatiotemporal CO_2 effect can be examined from the differences among the four simulations and the simulations (S1) based on the annual and uniformly distributed CO_2 data sets.

Integrated terrestrial ecosystem model

The integrated terrestrial ecosystem model (iTEM; Chen and Zhuang 2014, Liu et al. 2014) was designed for assessing spatially and temporally explicit CO_2 effects on the global carbon dynamics of terrestrial ecosystems. In iTEM, photosynthesis in C3 and C4 plants was simulated using Farquhar photosynthesis algorithm and Collatz et al. (1991) model, respectively. The leaf stomatal conductance, using the Ball-Berry model (Ball et al. 1987) scheme, was coupled to leaf photosynthesis in a similar manner to Collatz et al. (1992). The canopy was modeled in a one-layer, two-big-leaf approach

(Dai et al. 2004), which diagnosed energy budget, leaf temperature, evapotranspiration, and photosynthesis separately for sunlit and shaded leaves. The boundary layer turbulent processes were modeled based on the Monin–Obukhov Similarity Theory. The hydrological processes included the interception, through fall of precipitation, snow accumulation, sublimation and melt, surface runoff, surface evapotranspiration, water infiltration, and redistribution in soil and subsurface drainage. These algorithms allowed the model to simulate the response of land surface processes to changing environmental conditions. The iTEM has been calibrated and validated using various sources of observation data. Technical details of the iTEM were documented in Chen (2013).

We also used the biochemistry of C3 and C4 photosynthesis (A) coupled with a stomatal model to test the sensitivity of C3/C4 plant carbon assimilation to the atmospheric CO_2 variation. The photosynthesis algorithm adopted from Collatz et al. (1991, 1992) was used to calculate carbon uptake with relevant parameters (V_{max25}, maximum rate of carboxylation of Rubisco at 25°C) and considering environmental factors (boundary layer conductance, photosynthetic absorbed radiation, air temperature, relative humidity, and CO_2). Leaf photosynthesis was linked to stomatal conductance via the internal CO_2 concentration, which was calculated using Ball-Berry model scheme. The typical environmental conditions (e.g., ambient temperature) at growing season and corresponding photosynthetic and stomatal model parameters were (Appendix S1: Table S1) used to derive the A–C_a curve to quantify the sensitivity of photosynthesis to CO_2 variation.

Data

The high-precision CO_2 measurement from 2003 to 2004 at four typical flux tower sites including Howland forest main (US-Ho1) (evergreen forest, Hollinger et al. 1999), Missouri Ozark (US-Moz) (deciduous forest, Gu et al. 2006), LBA Tapajos KM67 Mature Forest (BR-Sa1) (tropical forest, Grant et al. 2009), and one cropland flux tower site, Mead Irrigated (US-Ne1) (Verma et al. 2005), was used. The flux tower sites characterized by grassland, savannas, and tundra were not selected, because forest is generally more sensitive to CO_2 variations (Ainsworth and Long 2005) and cropland has much larger photosynthetic capacity compared with other natural grassland ecosystems (Madani et al. 2014). We used the daytime averaged CO_2 mole fraction to account for the effects on photosynthesis for the summer season (June to September). To investigate the seasonal variability, we used a 31-d running mean to get a smooth CO_2 mole fraction daily daytime average data. In addition, the site-level tests were conducted using iTEM to compare the simulated daily GPP using in situ CO_2 observation with that using the uniformly distributed atmospheric CO_2 data. The micrometeorology data (e.g., radiation, wind, temperature) from the four flux sites above were used to drive the iTEM.

In global simulations, iTEM used spatially explicit data of climate, land cover, and soil. The details about the data sets of the vegetation (Appendix S1: Fig. S1) and soil texture can be found in Melillo et al. (1993) and Zhuang et al. (2003). The global simulations were applied at a spatial resolution of a 1° by 1° (longitude × latitude) for the global land area except the Antarctic. Forcing data including the radiation (direct, diffuse), the initial conditions, soil properties, the plant distribution, and vegetation-specific parameters as well as the 3-h meteorological data were from Chen and Zhuang (2014).

The explicitly spatial and seasonal CO_2 data from NOAA gridded CO_2 product (ftp://aftp.cmdl.noaa.gov/products/carbontracker/co2/) are based on global CO_2 observation network data obtained by employing a novel ensemble assimilation method to accurately model atmospheric CO_2 mole fractions (Peters et al. 2007). In the MACC project (https://www.gmes-atmosphere.eu/news/co2_forecasts/), atmospheric CO_2 concentration data are estimated by assimilating satellite observations into the ECMWF Integrated Forecasting System (IFS) Numerical Weather Prediction model. The global atmospheric CO_2 concentration is forecasted with a 5-d lead time at 3-h time step. Both spatially and temporally explicit CO_2 data sets were resampled to the spatial resolution of TEM. The annual and uniformly distributed CO_2 data sets for the period 2003–2010 were from ESRL data (http://www.esrl.noaa.gov/gmd/ccgg/trends/). Fig. 1 showed the spatial distributions of mean daytime CO_2 (9:00

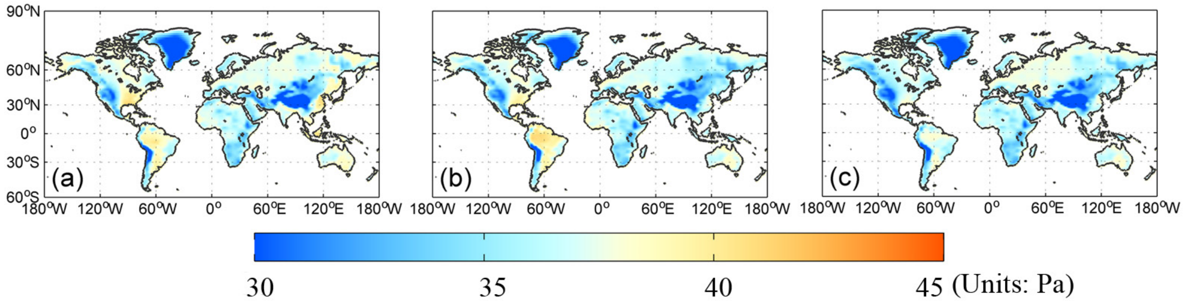

Fig. 1. The mean daytime CO_2 (9:00 to 15:00) partial pressure (Units: Pa) at summer (June to Sep) season during 2003–2010. (a–c) stand for the NOAA, MACC, and annual CO_2 partial pressure, respectively. Units: Pa.

to 15:00) partial pressure in these three products in summer (June to September) season during 2003–2010. Both NOAA CO_2 and MACC CO_2 (Fig. 1a, b) data sets indicated the CO_2 a large spatial variability with the value ranging from 30 to 42 Pa. Amazon and parts of China, and North America were characterized by higher CO_2 partial pressure (2–5 Pa) than the annual CO_2 data set, but Russia exhibited slightly lower partial pressure in summer season.

Results

CO_2 variation among sites and sensitivity test

All of the four sites exhibited a seasonal CO_2 variation, ranging from 0.8 to 3 Pa (Fig. 2). US-Ne1 had the largest seasonal amplitude (3 Pa), followed by US-Ho1 and US-Moz. In addition, the in situ CO_2 observation only showed slightly higher concentrations than the background CO_2 value at BR-Sa1. Spatially, the difference also reached as large as 2.5 Pa among these sites. For example, US-Ne1 had low CO_2 concentrations around 34 Pa at summer time in 2003, while in US-Ho1, the observed CO_2 was as high as 36.5 Pa. These high-precision CO_2 measurements showed that there were significant spatiotemporal surface CO_2 variations across sites. We derived the A–C_a curve for C3 and C4 plants (Fig. 3) using the coupled photosynthesis with stomatal model and the parameters in Appendix S1: Table S1. The slopes of A–C_a curve at 35 Pa CO_2 were around 0.3 μmol $CO_2 \cdot m^{-2} \cdot s^{-1} \cdot Pa^{-1}$ and 0.4 μmol $CO_2 \cdot m^{-2} \cdot s^{-1} \cdot Pa^{-1}$ for C3 and C4 plants, respectively. Therefore, the 2–3 Pa CO_2 differences could result in the difference of A about 0.6–0.9 μmol $CO_2 \cdot m^{-2} \cdot s^{-1}$ in C3 plant and 0.8–1.2 μmol $CO_2 \cdot m^{-2} \cdot s^{-1}$ in C4 plant, respectively.

Site-level test using in situ CO_2 observation

The CO_2 diurnal cycle exhibited negative effects on photosynthesis at US-Ho1, US-Moz, and US-Ne1 sites, but little positive effects on BR-Sa1 (Fig. 4). Although the fluctuating CO_2 showed higher partial pressure in spring, autumn, and winter seasons in temperate regions, the low temperature inhibited the plant carbon assimilations. For US-Moz and US-Ne1, the summer daytime CO_2 was about 2.5 Pa lower compared with the uniformly distributed atmospheric CO_2 data, with expected lower photosynthesis rates. Considering the realistic CO_2 temporal variation at US-Moz and US-Ne1, the annual GPP was 1334 g $C \cdot yr^{-1}$, 1245 g $C \cdot yr^{-1}$, respectively, which were about 3.8% lower than that in simulations using the uniformly distributed atmospheric CO_2 data.

Spatial and temporal CO_2 effects at the global scale

Using spatially and temporally explicit CO_2 data (S1-NOAA/S1-MACC), iTEM had lower annual GPP/NEP (−0.42 ± 0.06 Pg $C \cdot yr^{-1}$ for GPP and −0.10 ± 0.01 Pg $C \cdot yr^{-1}$ for NEP) estimation than that using the mean annual CO_2 value (S1-mNOAA/S1-mMACC), suggesting that CO_2 seasonal variation had negative effects on plant carbon assimilation (Fig. 5, Appendix S1: Fig. S2, Table 1). However, the global GPP/NEP, especially in temperate and tropical forest region, exhibited higher estimation (2.12 ± 0.11 Pg $C \cdot yr^{-1}$ for GPP and 0.18 ± 0.04 Pg $C \cdot yr^{-1}$ for NEP) when we only

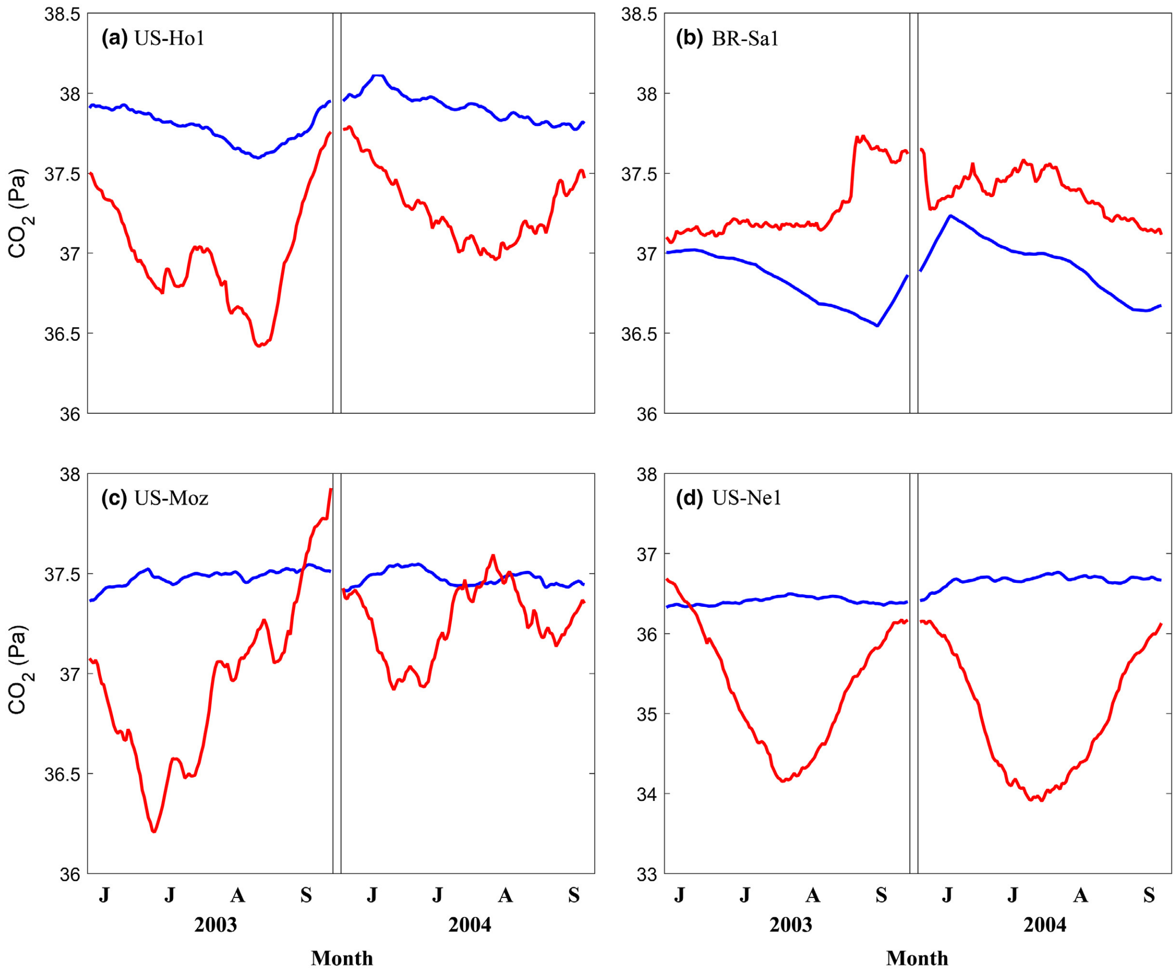

Fig. 2. Smoothed daily mean CO_2 partial pressure (red line) at four flux sites at growing seasons (June to September): (a) Howland forest main (US-Ho1), (b) LBA Tapajos KM67 Mature Forest (BR-Sa1), (c) Missouri Ozark and (US-Moz), and (d) Mead Irrigated (US-Ne1). The blue line stands for the monthly tropospheric "background" CO_2 concentration: see http://www.esrl.noaa.gov/gmd/cgg/trends.

considered the spatial CO_2 effect (Fig. 5, Appendix S1: Fig. S2, comparison between S1-mNOAA/S1-mMACC and S1). This indicated that surface mean annual CO_2 concentration was larger than the uniformly distributed CO_2 data sets. However, when both spatial and seasonal CO_2 effects were considered, GPP/NEP was slightly higher in tropical forest and temperate evergreen broadleaf forest, but lower in boreal forest compared with the simulation using the uniformly distributed CO_2 data sets (Fig. 5, Appendix S1: Fig. S2, comparison between S1-NOAA/S1-MACC and S1). All of three simulations suggested that forest showed relatively significant responses to the CO_2 variation (Fig. 5, Appendix S1: Fig. S2, Table S2). In addition, the comparison among the three simulations also showed strong seasonal variations (Fig. 6, Appendix S1: Fig. S3, we did not show the NEP comparison here). The effect of CO_2 seasonal variation on GPP was relatively obvious in summer season, with negative effect on the plant carbon sequestration. This was similar with the effect of CO_2 spatial variation, but with positive effects. It was noted that tropical forest responded to the CO_2 variation (seasonal or spatial) in all months.

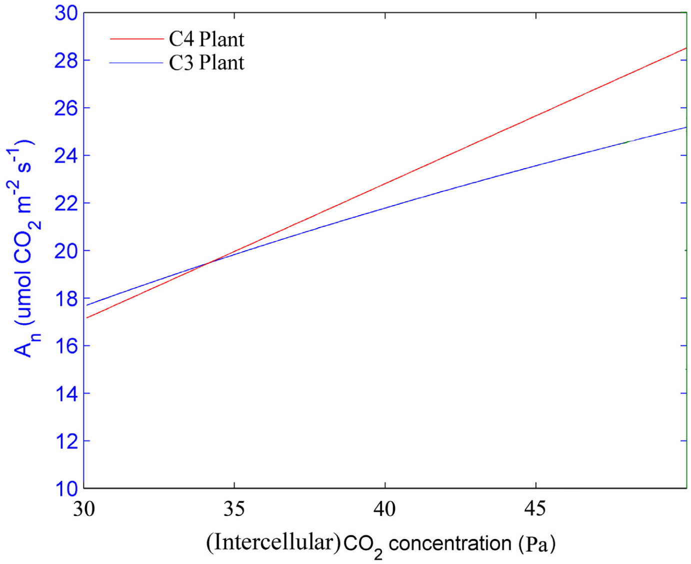

Fig. 3. The derived An-CO_2 curve in C3 and C4 plants using the biochemistry of C3 and C4 photosynthesis coupled with a stomatal model and assumption (environmental condition and parameters) in Appendix S1: Table S1.

Discussion

CO_2 spatial and temporal effects

Few previous site and regional studies considered the CO_2 temporal variations, most of which were conducted with a constant CO_2 value within a year. The study by Schurgers et al. (2015) used the vertical micrometeorological profile variations (light, relative humidity, and CO_2) within the canopy to address the importance of heterogeneous environmental conditions. Their results showed that only the light profile played an important role in photosynthesis and transpiration although large gradient CO_2 existed during early morning and stable night. Cardon et al. (1995) investigated the effects of fluctuating CO_2 concentrations with median level (340 ppmv) and average photosynthesis remained fairly constant under the oscillating CO_2. Although these studies indicated that the oscillating/diurnal cycle of CO_2 with median level (300–450 ppmv) may exhibit small effects on carbon uptake, both were conducted at short-term (few days) and the high frequent CO_2 fluctuation may not represent the natural CO_2 temporal variation. In our site-level test, the US-Moz and US-Ne1, characterized as lower CO_2 partial pressure in summer season, had lower GPP estimation (Fig. 4), suggesting a negative feedback on leaf photosynthesis. This was similar with the simulations using the mean annual CO_2 data set (Fig. 5, comparison between S1-NOAA and S1-mNOAA). Therefore, our results suggested that CO_2 seasonal variation had a negative impact on plant photosynthesis. Due to sparse surface CO_2 observation network (Shiga et al. 2013), the spatial CO_2 effects have rarely been studied in land surface models except some coupled land–atmosphere models (Nicholls et al. 2004, Lu et al. 2005, Combe et al. 2015). It should be noted that the annual background CO_2 data set (uniformly distributed CO_2 data set, simulation S1) was not the surface CO_2 which plant actually assimilates and may not correctly capture the global CO_2 spatial variations. The site-level CO_2 measurement (Fig. 2) and spatially, temporally explicit CO_2 data sets (Fig. 1) all indicated a large variation across the globe. Compared with the uniformly distributed CO_2 data set, some regions had similar value, but for tropical regions, the spatially, temporally explicit CO_2 data sets showed consistent higher concentrations than annual, uniformly distributed CO_2 (we only showed the summer daytime CO_2 in Fig. 1), thus resulted in higher annual GPP/NEP. This was consistent with the site-level test at the tropical site (BR-Sa1) (Figs. 2 and 4).

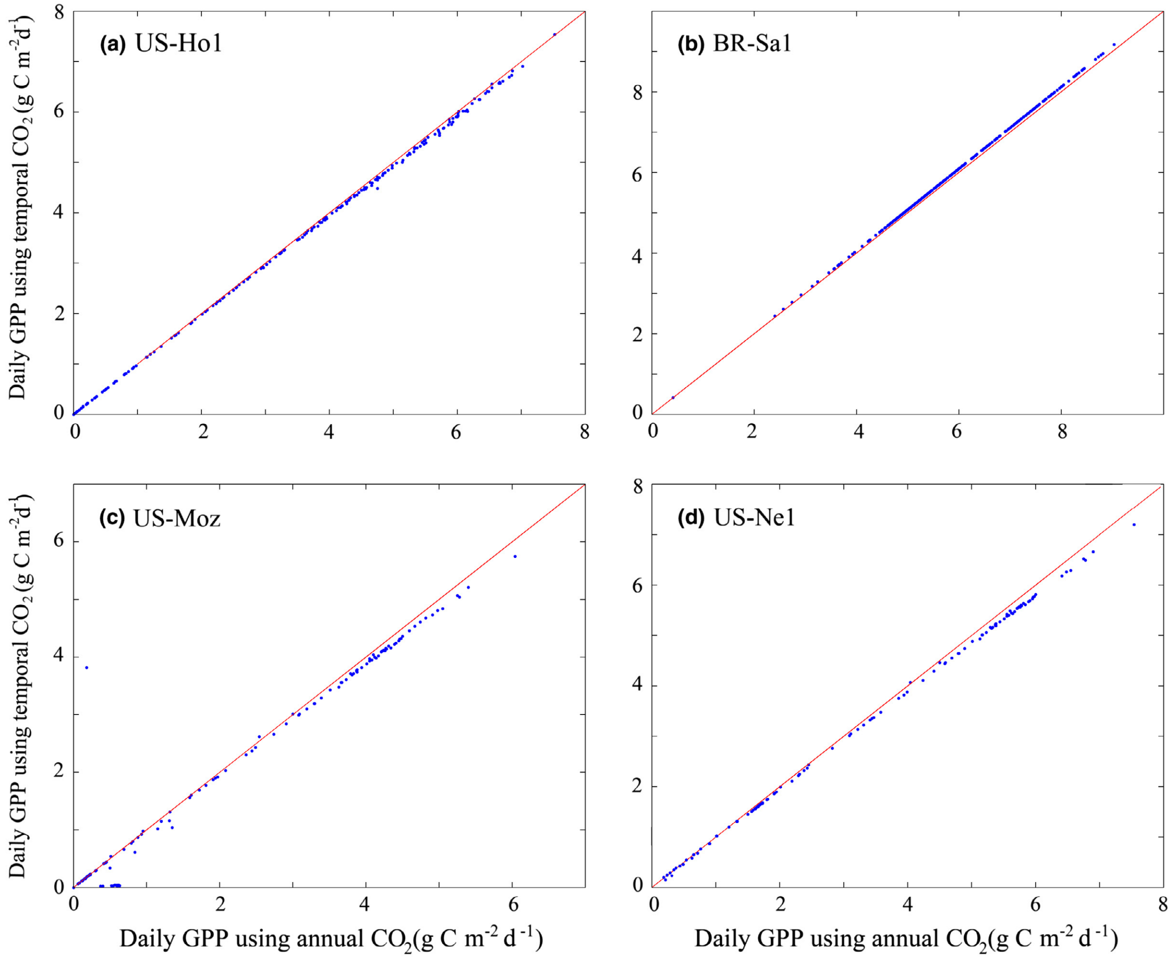

Fig. 4. Comparison between the simulated daily GPP using the in situ CO_2 observation with that using the annual CO_2 data sets at sites (a) Howland forest main (US-Ho1); (b) LBA Tapajos KM67 Mature Forest (BR-Sa1); (c) Missouri Ozark (US-Moz); and (d) Mead Irrigated (US-Ne1).

Accurate spatial and temporal CO_2 representations

We have to admit that the NOAA-CO_2 and MACC-CO_2 contained uncertainties and induced large biases to our global simulations. Both of the two spatially, temporally explicit CO_2 data exhibited higher values in the tropical regions. For example, the NOAA Carbon Tracker showed 1.5 Pa higher CO_2 partial pressure when compared with the uniformly distributed atmospheric CO_2 data (Appendix S1: Fig. S4), while the in situ CO_2 observation only exhibits 0.5 Pa differences at the BR-Sa1 site (Fig. 2b). In addition, the seasonal variation in NOAA Carbon Tracker was also different from the in situ CO_2 observation in temperate regions: the in situ observed CO_2 partial pressure was generally lower in summer season (Fig. 2a, c, d), but the NOAA Carbon Tracker had similar CO_2 partial pressure with the uniformly distributed atmospheric CO_2 (Appendix S1: Fig. S4a, c, d). The discrepancy between the in situ CO_2 observation and NOAA Carbon Tracker could be due to the following reasons. First, NOAA Carbon Tracker is a global inverse model, whose accuracy is highly dependent on the prior CO_2 fluxes. Second, the global inversion lacks an explicit crop model and explicit subdaily prediction of carbon exchanges. Finally, the transport model (TM5) used in NOAA Carbon Tracker is based on a relatively coarse spatial resolution, which limits the ability to simulate the CO_2 transport due to inaccurate weather data in

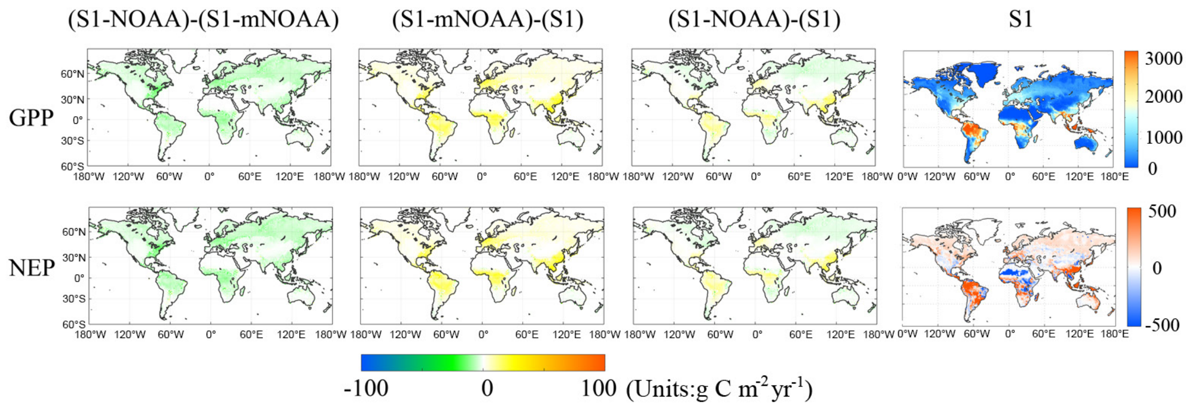

Fig. 5. Temporal averaged GPP and NEP differences from 2003 to 2010. The first column is the difference between S1-NOAA and S1-mNOAA, the second column is the difference between S1-mNOAA and S1, and the third column is the difference between S1-NOAA and S1. S1 stands for the iTem simulation using the uniformly distributed atmospheric CO_2, S1-mNOAA means the simulation using mean annual CO_2 computed from NOAA-CO_2 data, and S1-NOAA means the simulations using CO_2 from NOAA-CO_2 data. Units: g C·m^{-2}·yr^{-1}.

complex terrain (Geels et al. 2007). Our simulations showed that spatially/temporally varied atmospheric CO_2 exerted relatively significant effects on the global carbon dynamics, especially in forest regions. However, the spatially and temporally explicit CO_2 product used here might be biased due to sparse monitoring network (Peters et al. 2007) and measurement errors (Masarie et al. 2011). Thus, high frequency, stable CO_2 measurement (Andrews et al. 2014) and more CO_2 observation sites capturing seasonal/spatial variation representative of large regions (Bakwin et al. 2004, Lauvaux et al. 2012) are needed to constrain estimates of regional/global net atmosphere/biosphere exchange of CO_2.

Implications for future studies

Up to now, most of the regional and global estimations of terrestrial carbon uptake come from various ecosystem land surface models (Bonan 2008). The model constrained with eddy flux tower observation would strengthen the understanding of ecosystem mechanisms. The data-assimilation method provides an alternative way to quantifying regional carbon exchanges between the terrestrial biosphere and the atmosphere at continental and global scales (Xiao et al. 2012). Generally, in the land surface models, using CO_2 data as input to compute GPP, the carbon fluxes are routinely simulated based on annual, uniformly distributed CO_2 data set (or to be more specific, the background CO_2 concentration; our study was the simulation S1) across a region or globe (Turner et al. 2003, Chen et al. 2011), without considering the site-level CO_2 realistic properties (Liu et al. 2016). As we demonstrated above, the high-precision CO_2 measurement from eddy flux towers showed that seasonal and spatial surface atmospheric CO_2 concentration differences were as large as 35 ppmv. Using the sensitivity analysis, the seasonal and spatial gradient can

Table 1. Annual global GPP and NEP estimation.

Measurement	S1	S1-mNOAA	S1-NOAA	S1-mMACC	S1-MACC
Annual GPP (Pg C·yr^{-1}) flux	128.82 ± 4.12	128.43 ± 4.17	130.56 ± 4.09	128.37 ± 4.07	130.48 ± 4.09
Cumulative NEP (Pg C) flux	47.41	46.62	48.89	46.63	48.85

Notes: S1 stands for the iTem simulation using the uniformly distributed atmospheric CO_2, S1-mNOAA means the simulation using mean annual CO_2 computed from NOAA-CO_2 data, and S1-NOAA means the simulations using CO_2 from NOAA-CO_2 data. S1-mMACC means the simulation using mean annual CO_2 computed from NOAA-CO_2 data, and S1-MACC means the simulations using CO_2 from NOAA-CO_2 data. Annual GPP values are presented as mean ± SE.

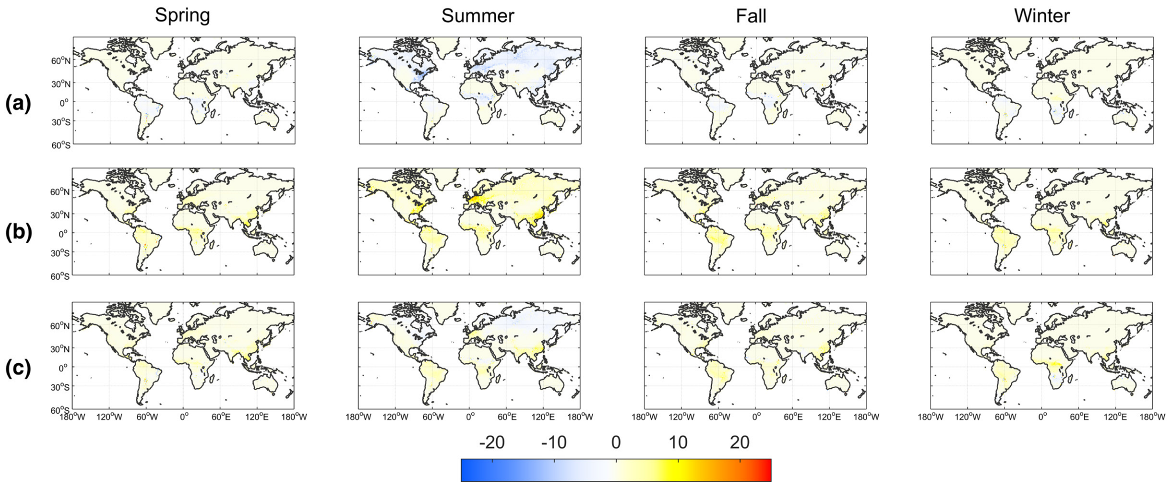

Fig. 6. Seasonal averaged GPP differences among S1-NOAA, S1-mNOAA, and S1 (S1, S1-mNOAA, and S1-NOAA stand for the iTEM simulations using the uniformly distributed atmospheric CO_2 (a), mean annual CO_2 computed from NOAA-CO_2 (b), and NOAA-CO_2 data (c), respectively. Units: g $C \cdot m^{-2} \cdot season^{-1}$).

induce around 0.6–1.2 μmol $CO_2 \cdot m^{-2} \cdot s^{-1}$ differences in photosynthesis (Fig. 3). We should note that the photosynthesis in C3 plant was prone to be saturated at high CO_2 concentrations and this difference could be small in future climate scenarios. However, the seasonal CO_2 amplitude is expected to increase as indicated by the fifth phase of the Coupled Model Intercomparison Project (CMIP5) (Zhao and Zeng 2014), which could still result in significant differences in photosynthesis.

As for the model scheme, we should also pay attention to the oscillation of elevated CO_2 effects on plant carbon assimilation. Some studies were conducted on the fluctuation of elevated CO_2 effects on photosynthesis when compared with the constant CO_2 experiments (similar to the annual CO_2 in this study). Hendrey et al. (1997) exposed the wheat to elevated CO_2 (650 ppmv) oscillating symmetrically 225 ppmv and the results showed that carbon uptake was decreased if the duration of oscillation was more than 1 min. This downregulation of photosynthesis was confirmed by other similar studies (Chaves et al. 2001, Holtum and Winter 2003, Bunce 2012). The artificially controlled CO_2 oscillation may not be representative of natural CO_2 diurnal/seasonal variations, and the response to rapid changes in ambient CO_2 by the experiments above indicates that plant may acclimate to the elevated CO_2 diurnal cycle. In addition, the biogeochemical processes, such as the C and N interaction, allocation, turnover scheme (Friedlingstein et al. 2014, Zaehle et al. 2014, Walker et al. 2015), and the heat- or drought-induced mortality mechanism (Williams 2014, Williams et al. 2014, Yi et al. 2015), are needed to be better represented in land surface models to accurately capture the plant response to a warmer and CO_2 richer future.

Conclusion

Atmospheric CO_2 is an important factor related to plant carbon assimilation and water balance. Current ecosystem models have not explored the atmospheric CO_2 effects in a spatially and temporally explicit manner. Our analysis indicated that there were significant differences in seasonal and spatial CO_2 concentrations at various eddy flux tower sites (up to 35 ppmv), which could result in 3–8% differences in photosynthesis rate. Our results demonstrated that CO_2 seasonal variations had a negative effect on plant carbon assimilation, while CO_2 spatial variation exhibited positive impacts. When both CO_2 seasonal and spatial effects were considered, global GPP and net ecosystem production (NEP) were 1.7 Pg $C \cdot yr^{-1}$ and 0.08 Pg $C \cdot yr^{-1}$ higher than the simulation using uniformly distributed CO_2 data set and the difference was significant in tropical and temperate evergreen broadleaf forest regions. This study suggests that using spatially and temporally explicit atmospheric CO_2 data are important to accurately quantifying the regional and global carbon dynamics of terrestrial ecosystems and the observation network should be expanded to have a representative CO_2 surface variation.

Acknowledgments

The model forcing data are provided by the Land Surface Hydrology Research Group at Princeton University. This research is funded through projects to Q.Z. by NASA Land Use and Land Cover Change program (NASA-NNX09A126G), Department of Energy (DE-FG02-08ER64599), National Science Foundation (NSF-102891 and NSF-0919331), NSF Carbon and Water in the Earth Program (NSF-0630319), and NSF CDI Type II project (IIS-1028291).

Literature Cited

Ainsworth, E. A., and S. P. Long. 2005. What have we learned from 15 years of free-air CO_2 enrichment (FACE)? A meta-analytic review of the responses of photosynthesis, canopy properties and plant production to rising CO_2. New Phytologist 165:351–372.

Andrews, A., J. Kofler, M. Trudeau, J. Williams, D. Neff, K. Masarie, D. Chao, D. Kitzis, P. Novelli, and C. Zhao. 2014. CO_2, CO, and CH_4 measurements from tall towers in the NOAA Earth System Research Laboratory's Global Greenhouse Gas Reference Network: instrumentation, uncertainty analysis, and recommendations for future high-accuracy greenhouse gas monitoring efforts. Atmospheric Measurement Techniques 7:647–687.

Bakwin, P. S., K. J. Davis, C. Yi, S. C. Wofsy, J. W. Munger, L. Haszpra, and Z. Barcza. 2004. Regional carbon dioxide fluxes from mixing ratio data. Tellus 56B:301–311.

Ball, J., T. Woodrow, and J. Berry. 1987. A model predicting stomatal conductance and its contribution to the control of photosynthesis under different environmental conditions. Progress in Photosynthesis Research 4:221–224.

Bonan, G. B. 2008. Forests and climate change: forcings, feedbacks, and the climate benefits of forests. Science 320:1444–1449.

Bunce, J. A. 2012. Responses of cotton and wheat photosynthesis and growth to cyclic variation in carbon dioxide concentration. Photosynthetica 50:395–400.

Canadell, J. G., C. Le Quéré, M. R. Raupach, C. B. Field, E. T. Buitenhuis, P. Ciais, T. J. Conway, N. P. Gillett, R. Houghton, and G. Marland. 2007. Contributions to accelerating atmospheric CO_2 growth from economic activity, carbon intensity, and efficiency of natural sinks. Proceedings of the National Academy of Sciences USA 104:18866–18870.

Cardon, Z. G., J. A. Berry, and I. E. Woodrow. 1995. Fluctuating CO_2 drives species-specific changes in water use efficiency. Journal of Biogeography 22:203–208.

Chahine, M., L. Chen, P. Dimotakis, X. Jiang, Q. Li, E. T. Olsen, T. Pagano, J. Randerson, and Y. L. Yung. 2008. Satellite remote sounding of mid-tropospheric CO_2. Geophysical Research Letters 35:179–190.

Chaves, M. M., E. Pantschitz, and E. D. Schulze. 2001. Growth and photosynthetic carbon metabolism in tobacco plants under an oscillating CO_2 concentration in the atmosphere. Plant Biology 3:417–425.

Chen, M. 2013. Evaluation of atmospheric aerosol and tropospheric ozone effects on global terrestrial ecosystem carbon dynamics, Purdue University. ProQuest Dissertations and Theses, 225. http://search.proquest.com/docview/1433825784? accountid=13360

Chen, M., and Q. Zhuang. 2014. Evaluating aerosol direct radiative effects on global terrestrial ecosystem carbon dynamics from 2003 to 2010. Tellus Series B 66:21808.

Chen, M., Q. Zhuang, Q. Cook, D. R. Coulter, R. Pekour, M. Scott, R. L. Munger, and K. Bible. 2011. Quantification of terrestrial ecosystem carbon dynamics in the conterminous United States combining a process-based biogeochemical model and MODIS and AmeriFlux data. Biogeosciences 8:2665–2688.

Collatz, G. J., J. T. Ball, C. Grivet, and J. A. Berry. 1991. Physiological and environmental regulation of stomatal conductance, photosynthesis and transpiration: a model that includes a laminar boundary layer. Agricultural and Forest Meteorology 54:107–136.

Collatz, G. J., M. Ribas-Carbo, and J. A. Berry. 1992. Coupled photosynthesis-stomatal conductance model for leaves of C4 plants. Functional Plant Biology 19:519–538.

Combe, M., J. Vilà-Guerau de Arellano, H. G. Ouwersloot, C. M. J. Jacobs, and W. Peters. 2015. Two perspectives on the coupled carbon, water and energy exchange in the planetary boundary layer. Biogeosciences 12:103–123.

Dai, Y., R. E. Dickinson, and Y.-P. Wang. 2004. A two-big-leaf model for canopy temperature, photosynthesis, and stomatal conductance. Journal of Climate 17:2281–2299.

Davis, K. J., P. S. Bakwin, C. Yi, B. W. Berger, C. Zhao, R. M. Teclaw, and J. Isebrands. 2003. The annual cycles of CO_2 and H_2O exchange over a northern mixed forest as observed from a very tall tower. Global Change Biology 9:1278–1293.

Eby, M., K. Zickfeld, A. Montenegro, D. Archer, K. Meissner, and A. Weaver. 2009. Lifetime of anthropogenic climate change: millennial time scales of potential CO_2 and surface temperature perturbations. Journal of Climate 22:2501–2511.

Esser, G., and M. Lautenschlager. 1994. Estimating the change of carbon in the terrestrial biosphere from 18 000 BP to present using a carbon cycle model. Environmental Pollution 83:45–53.

Feng, L., P. I. Palmer, Y. Yang, R. M. Yantosca, S. R. Kawa, J.-D. Paris, H. Matsueda, and T. Machida. 2011. Evaluating a 3-D transport model of atmospheric CO_2 using ground-based, aircraft, and space-borne data. Atmospheric Chemistry and Physics 11:2789–2803.

Friedlingstein, P., M. Meinshausen, V. K. Arora, C. D. Jones, A. Anav, S. K. Liddicoat, and R. Knutti. 2014. Uncertainties in CMIP5 climate projections due to carbon cycle feedbacks. Journal of Climate 27:511–526.

Geels, C., M. Gloor, P. Ciais, P. Bousquet, P. Peylin, A. Vermeulen, R. Dargaville, T. Aalto, J. Brandt, and J. Christensen. 2007. Comparing atmospheric transport models for future regional inversions over Europe-Part 1: mapping the atmospheric CO_2 signals. Atmospheric Chemistry and Physics 7:3461–3479.

Gerber, S., F. Joos, and I. C. Prentice. 2004. Sensitivity of a dynamic global vegetation model to climate and atmospheric CO_2. Global Change Biology 10:1223–1239.

Grant, R. F., L. R. Hutyra, R. C. Oliveira, J. W. Munger, S. R. Saleska, and S. C. Wofsy. 2009. Modeling the carbon balance of Amazonian rain forests: resolving ecological controls on net ecosystem productivity. Ecological Monographs 79:445–463.

Gu, L., T. Meyers, S. G. Pallardy, P. J. Hanson, B. Yang, M. Heuer, K. P. Hosman, J. S. Riggs, D. Sluss, and S. D. Wullschleger. 2006. Direct and indirect effects of atmospheric conditions and soil moisture on surface energy partitioning revealed by a prolonged drought at a temperate forest site. Journal of Geophysical Research 111:102. http://dx.doi.org/10.1029/2006JD007161

Haszpra, L., Z. Barcza, D. Hidy, I. Szilágyi, E. Dlugokencky, and P. Tans. 2008. Trends and temporal variations of major greenhouse gases at a rural site in Central Europe. Atmospheric Environment 42:8707–8716.

Hendrey, G. R., S. P. Long, I. F. McKee, and N. R. Baker. 1997. Can photosynthesis respond to short-term fluctuations in atmospheric carbon dioxide? Photosynthesis Research 51:179–184.

Hollinger, D. Y., S. M. Goltz, E. A. Davidson, J. T. Lee, K. Tu, and H. T. Valentine. 1999. Seasonal patterns and environmental control of carbon dioxide and water vapor exchange in an ecotonal boreal forest. Global Change Biology 5:891–902.

Holtum, J. A., and K. Winter. 2003. Photosynthetic CO_2 uptake in seedlings of two tropical tree species exposed to oscillating elevated concentrations of CO_2. Planta 218:152–158.

Krinner, G., N. Viovy, N. de Noblet-Ducoudré, J. Ogée, J. Polcher, P. Friedlingstein, P. Ciais, S. Sitch, and I. C. Prentice. 2005. A dynamic global vegetation model for studies of the coupled atmosphere-biosphere system. Global Biogeochemical Cycles 19:GB1015. http://dx.doi.org/10.1029/2003GB002199

Lauvaux, T., A. E. Schuh, M. Bocquet, L. Wu, S. Richardson, N. Miles, and K. J. Davis. 2012. Network design for mesoscale inversions of CO_2 sources and sinks. Tellus Series B 64:5275–5308.

Lawrence, D. M., K. W. Oleson, M. G. Flanner, P. E. Thornton, S. C. Swenson, P. J. Lawrence, X. Zeng, Z. L. Yang, S. Levis, and K. Sakaguchi. 2011. Parameterization improvements and functional and structural advances in version 4 of the Community Land Model. Journal of Advances in Modeling Earth Systems 3:365–375.

Liu, S., M. Chen, and Q. Zhuang. 2014. Aerosol effects on global land surface energy fluxes during 2003–2010. Geophysical Research Letters 41:7875–7881.

Liu, S., Q. Zhuang, Y. He, A. Noormets, J. Chen, and L. Gu. 2016. Evaluating atmospheric CO_2 effects on gross primary productivity and net ecosystem exchanges of terrestrial ecosystems in the conterminous United States using the AmeriFlux data and an artificial neural network approach. Agricultural and Forest Meteorology 220:38–49.

Long, S. P., E. A. Ainsworth, A. Rogers, and D. R. Ort. 2004. Rising atmospheric carbon dioxide: plants FACE the future. Annual Review of Plant Biology 55:591–628.

Lu, L., A. S. Denning, M. A. da Silva-Dias, P. da Silva-Dias, M. Longo, S. R. Freitas, and S. Saatchi. 2005. Mesoscale circulations and atmospheric CO_2 variations in the Tapajós Region, Pará, Brazil. Journal of Geophysical Research 110:2927–2934.

Madani, N., J. S. Kimball, D. L. R. Affleck, J. Kattge, J. Graham, P. M. Bodegom, P. B. Reich, and S. W. Running. 2014. Improving ecosystem productivity modeling through spatially explicit estimation of optimal light use efficiency. Journal of Geophysical Research 119:1755–1769.

Masarie, K., G. Pétron, A. Andrews, L. Bruhwiler, T. Conway, A. Jacobson, J. Miller, P. Tans, D. Worthy, and W. Peters. 2011. Impact of CO_2 measurement bias on CarbonTracker surface flux estimates. Journal of Geophysical Research 116:1161–1166.

McGuire, A., L. Joyce, D. Kicklighter, J. Melillo, G. Esser, and C. Vorosmarty. 1993. Productivity response of climax temperate forests to elevated temperature and carbon dioxide: a North American comparison between two global models. Climatic Change 24:287–310.

Melillo, J. M., A. D. McGuire, D. W. Kicklighter, B. Moore, C. J. Vorosmarty, and A. L. Schloss. 1993. Global climate change and terrestrial net primary production. Nature 363:234–240.

Miles, N. L., S. J. Richardson, K. J. Davis, T. Lauvaux, A. E. Andrews, T. O. West, V. Bandaru, and E. R. Crosson. 2012. Large amplitude spatial and temporal gradients in atmospheric boundary layer CO_2 mole fractions detected with a tower-based network in the US upper Midwest. Journal of Geophysical Research 117:72–84.

Nicholls, M. E., A. S. Denning, L. Prihodko, P. L. Vidale, I. Baker, K. Davis, and P. Bakwin. 2004. A multiple-scale simulation of variations in atmospheric carbon dioxide using a coupled biosphere-atmospheric model. Journal of Geophysical Research 109:1933–1943.

Norby, R. J., and D. R. Zak. 2011. Ecological lessons from free-air CO_2 enrichment (FACE) experiments. Annual Review of Ecology, Evolution, and Systematics 42:181.

Norby, R. J., P. J. Hanson, E. G. O'Neill, T. J. Tschaplinski, J. F. Weltzin, R. A. Hansen, W. Cheng, S. D. Wullschleger, C. A. Gunderson, and N. T. Edwards. 2002. Net primary productivity of a CO_2-enriched deciduous forest and the implications for carbon storage. Ecological Applications 12:1261–1266.

Oleson, K. W., D. M. Lawrence, B. Gordon, M. G. Flanner, E. Kluzek, J. Peter, S. Levis, S. C. Swenson, E. Thornton, and J. Feddema. 2010. Technical description of version 4.0 of the Community Land Model (CLM). http://www.cesm.ucar.edu/models/cesm1.0/clm/CLM4_Tech_Note.pdf

Pan, Y., J. M. Melillo, A. D. McGuire, D. W. Kicklighter, L. F. Pitelka, K. Hibbard, L. L. Pierce, S. W. Running, D. S. Ojima, and W. J. Parton. 1998. Modeled responses of terrestrial ecosystems to elevated atmospheric CO_2: a comparison of simulations by the biogeochemistry models of the Vegetation/Ecosystem Modeling and Analysis Project (VEMAP). Oecologia 114:389–404.

Peters, W., A. R. Jacobson, C. Sweeney, A. E. Andrews, T. J. Conway, K. Masarie, J. B. Miller, L. M. Bruhwiler, G. Petron, and A. I. Hirsch. 2007. An atmospheric perspective on North American carbon dioxide exchange: CarbonTracker. Proceedings of the National Academy of Sciences USA 104:18925–18930.

Raich, J., E. Rastetter, J. Melillo, D. Kicklighter, P. Steudler, B. Peterson, A. Grace, B. Moore Iii, and C. Vorosmarty. 1991. Potential net primary productivity in South America: application of a global model. Ecological Applications 1:399–429.

Ruzmaikin, A., H. H. Aumann, and T. S. Pagano. 2012. Patterns of CO_2 variability from global satellite data. Journal of Climate 25:6383–6393.

Schurgers, G., F. Lagergren, M. Mölder, and A. Lindroth. 2015. The importance of micrometeorological variations for photosynthesis and transpiration in a boreal coniferous forest. Biogeosciences 12:237–256.

Shiga, Y. P., A. M. Michalak, S. Randolph Kawa, and R. J. Engelen. 2013. In-situ CO_2 monitoring network evaluation and design: a criterion based on atmospheric CO_2 variability. Journal of Geophysical Research 118:2007–2018.

Sitch, S., B. Smith, I. C. Prentice, A. Arneth, A. Bondeau, W. Cramer, J. Kaplan, S. Levis, W. Lucht, and M. T. Sykes. 2003. Evaluation of ecosystem dynamics, plant geography and terrestrial carbon cycling in the LPJ dynamic global vegetation model. Global Change Biology 9:161–185.

Turner, D. P., W. D. Ritts, W. B. Cohen, S. T. Gower, M. Zhao, S. W. Running, S. C. Wofsy, S. Urbanski, A. L. Dunn, and J. Munger. 2003. Scaling gross primary production (GPP) over boreal and deciduous forest landscapes in support of MODIS GPP product validation. Remote Sensing of Environment 88:256–270.

Verma, S. B., A. Dobermann, and K. G. Cassman. 2005. Annual carbon dioxide exchange in irrigated and rainfed maize-based agroecosystems. Agricultural and Forest Meteorology 131:77–96.

Walker, A. P., et al. 2015. Predicting long-term carbon sequestration in response to CO_2 enrichment: How and why do current ecosystem models differ? Global Biogeochemical Cycles 29:476–495.

White, M. A., P. E. Thornton, S. W. Running, and R. R. Nemani. 2000. Parameterization and sensitivity analysis of the BIOME-BGC terrestrial ecosystem model: net primary production controls. Earth Interactions 4:1–85.

Williams, C. A. 2014. Heat and drought extremes likely to stress ecosystem productivity equally or more in a warmer, CO_2 rich future. Environmental Research Letters 9:101002–101005.

Williams, I. N., M. S. Torn, W. J. Riley, and M. F. Wehner. 2014. Impacts of climate extremes on gross primary production under global warming. Environmental Research Letters 9:094011.

Xiao, J., J. Chen, K. J. Davis, and M. Reichstein. 2012. Advances in upscaling of eddy covariance measurements of carbon and water fluxes. Journal of Geophysical Research 117:1–4.

Yang, Z., G. C. Toon, J. S. Margolis, and P. O. Wennberg. 2002. Atmospheric CO_2 retrieved from ground-based near IR solar spectra. Geophysical Research Letters 29:53-1–53-4.

Yi, C., K. J. Davis, P. S. Bakwin, B. W. Berger, and L. Marr. 2000. The influence of advection on measurements of the net ecosystem-atmosphere exchange of CO_2 from a very tall tower. Journal of Geophysical Research 105:9991–9999.

Yi, C., K. J. Davis, P. S. Bakwin, A. S. Denning, N. Zhang, A. Desai, J. C. Lin, and C. Gerbig. 2004. The observed covariance between ecosystem carbon exchange and atmospheric boundary layer dynamics at a site in northern Wisconsin. Journal of Geophysical Research 109:D08302.

Yi, C., E. Pendall, and P. Ciais. 2015. Focus on extreme events and the carbon cycle. Environmental Research Letters 10:070201.

Yokota, T., Y. Yoshida, N. Eguchi, Y. Ota, T. Tanaka, H. Watanabe, and S. Maksyutov. 2009. Global concentrations of CO_2 and CH_4 retrieved from GOSAT: first preliminary results. Sola 5:160–163.

Zaehle, S., et al. 2014. Evaluation of 11 terrestrial carbon–nitrogen cycle models against observations from two temperate free-air CO_2 enrichment studies. New Phytologist 202:803–822.

Zeng, N., F. Zhao, G. J. Collatz, E. Kalnay, R. J. Salawitch, T. O. West, and L. Guanter. 2014. Agricultural green revolution as a driver of increasing atmospheric CO_2 seasonal amplitude. Nature 515:394–397.

Zhao, F., and N. Zeng. 2014. Continued increase in atmospheric CO_2 seasonal amplitude in the 21st century projected by the CMIP5 Earth system models. Earth System Dynamics 5:423–439.

Zhuang, Q., A. McGuire, J. Melillo, J. Clein, R. Dargaville, D. Kicklighter, R. Myneni, J. Dong, V. Romanovsky, and J. Harden. 2003. Carbon cycling in extratropical terrestrial ecosystems of the Northern Hemisphere during the 20th century: a modeling analysis of the influences of soil thermal dynamics. Tellus Series B 55:751–776.

Supporting Information

Additional Supporting Information may be found online at: http://onlinelibrary.wiley.com/doi/10.1002/ecs2.1391/supinfo